

1 Numerical Assessment of EMF Exposure of a Cow to a Wireless Power Transfer

2 System for Dairy Cattle

3 *Computers and Electronics in Agriculture, 151, (2018) 219-225.*

4

5 Said Benaissa<sup>a, b,\*</sup>, Amine M. Samoudi<sup>a</sup>, David Plets<sup>a</sup>, Günter Vermeeren<sup>a</sup>, Leen Verloock<sup>a</sup>, Ben  
6 Minnaert<sup>c</sup>, Nobby Stevens<sup>c</sup>, Luc Martens<sup>a</sup>, Frank A.M. Tuytens<sup>b, d</sup>, Bart Sonck<sup>b, e</sup>, Wout Joseph<sup>a</sup>

7 <sup>a</sup> Department of Information Technology, Ghent University/imec, Technologiepark-Zwijnaarde 15, 9052 Ghent, Belgium

8 <sup>b</sup> Flanders Research Institute for Agriculture, Fisheries and Food (ILVO). Animal Sciences Unit, Scheldeweg 68, 9090 Melle, Belgium

9 <sup>c</sup> Faculty of Engineering Technology, DraMCo Research Group, ESAT, KU Leuven, Ghent, Belgium

10 <sup>d</sup> Department of Nutrition, Genetics and Ethology, Faculty of Veterinary Medicine, Heidestraat 19, B-9820 Merelbeke, Belgium

11 <sup>e</sup> Department of Animal production, Faculty of Bioscience Engineering, Ghent University, Coupure links 653, B-9000 Ghent, Belgium

12 \* Corresponding author: Said Benaissa, Tel.: +32 09 331 48 60; E-mail address: [said.benaissa@ugent.be](mailto:said.benaissa@ugent.be)

13

14 **Abstract**

15 In this paper, we assessed the exposure of a cow to the electromagnetic fields (EMFs) induced by a  
16 wireless power transfer (WPT) system working at 92 kHz in a dairy barn. Cow exposure to the  
17 radiated EMFs was evaluated and compared to safety guidelines. We modeled a realistic WPT system  
18 for dairy cows in Sim4Life, a 3D electromagnetic simulation tool. We validated the model with  
19 electric field measurements; simulated fields deviated on average 6% from measured fields. We used  
20 the proposed WPT model to evaluate the stimulation and thermal effects based on the internal  
21 electric field and the specific absorption rate (SAR), respectively. Results showed that the exposure  
22 mainly varied with the distance of the transmitter to the body: variation of 5 dB of the induced  
23 electric field when the transmitter was set at 20 cm and 10 cm from the body. The distance of the  
24 receiver to the body influenced the exposure less (10%). We also compared the exposure with the  
25 limits provided by the International Commission on Non-Ionizing Radiation Protection (ICNIRP). The

26 internal electric fields were more conservative than SAR, which showed values far below exposure  
27 limits.

## 28 **Keywords**

29 Dairy health monitoring, precision livestock farming (PLF), wireless power transfer, electromagnetic  
30 exposure, induced electric field, specific absorption rate (SAR), internet-of-animals

31

## 32 **1. Introduction**

33 The continuous demand for increased production and the efforts for minimizing the environmental  
34 impact and saving costs make cattle monitoring using on-cow sensors widely adopted in today's dairy  
35 farms (Andersson et al., 2016; Benaissa et al., 2016a, 2016b; González et al., 2015; Neethirajan, 2017;  
36 Rutten et al., 2017; Van Nuffel et al., 2015). As sensor nodes are generally battery-powered devices  
37 with low processing and storage capabilities, the critical aspects to face are how to increase the  
38 battery capacity, reduce the energy consumption of nodes and avoid frequent battery replacement.  
39 Energy harvesting methods for wearable devices have emerged as an attractive solution to overcome  
40 the power consumption challenges (Minnaert et al., 2017). Energy could be harvested using passive  
41 sources from motion and vibration, solar energy, and ambient radio frequency (RF) energy  
42 (Bhatnagar and Owende, 2015). Although the sources are often available, the amount of power  
43 harvested is in the micro-watt range, which is insufficient to operate RF wireless transceiver modules  
44 in wearable devices (Nguyen et al., 2015). On the other hand, active energy sources involve wireless  
45 power transmission (WPT) coils to supply power to wearable devices. WPT can be conveniently  
46 optimized to satisfy power supply requirements. Moreover, WPT facilitates long term cow  
47 monitoring, as it allows an easy optimization of power supply, eliminates frequent battery  
48 replacement and reduces the weight and size of the wearable sensor (Minnaert et al., 2017).

49 However, the integration of WPT components would generate electromagnetic fields (EMF) in the  
50 proximity of the cow. Therefore, it is necessary to characterize EMF induced in the cow's body by a  
51 WPT system in a dairy barn. Effects of other EMF sources on cows (i.e., RF, stray voltage, extremely  
52 low frequency (ELF) electric and magnetic fields) have been frequently discussed in journals and  
53 meetings with agricultural, veterinary or dairy backgrounds (Algers and Hultgren, 1987; Burchard et

54 al., 1998; Burda et al., 2009; Hillman et al., 2013). For instance, Löscher (2003) reported that dairy  
55 cows exposed to TV and radio transmitting antennas showed reduced milk yield, health problems  
56 (e.g. avoidance behavior, poor general condition), and behavioral abnormalities (Löscher, 2003). In  
57 addition, Erdreich et al. (2009) did not observe any indications that bovine production and behavior  
58 were affected by exposure to up to 3 mA of stray voltage at 50 or 60 Hz for up to 3 or 4 weeks.  
59 However, Hillman et al. (2013) found that not only the cows' behavior, but also health and milk  
60 production were negatively affected by stray voltage fields. Moreover, Burchard et al. (1998)  
61 concluded that exposure to ELF EMF (i.e., 60 Hz, 10 kV/m, 30  $\mu$ T) for several 28-day-periods had no  
62 effects on cow progesterone levels. Although, the exposed animals had a prolonged estrous cycle.  
63 None of these studies has provided numerical or experimental estimates of cow exposure to EMF.  
64 Also, no work has investigated the electromagnetic effect of WPT system on the cow's body.  
65 Therefore, the aim of this work was to numerically model a realistic WPT system for dairy cows using  
66 a 3-D electromagnetic solver (Sim4Life), to validate the proposed model with experiments, to assess  
67 the cow's exposure to the radiated EMF by calculating the internal electric field and the SAR, and to  
68 compare the results with the safety exposure guidelines. We compared cow exposure to EMF with  
69 guidelines for human exposure, as, to date, no guidelines exist for animal exposure to EMF. For  
70 human exposure, international bodies like the International Commission on Non-Ionizing Radiation  
71 Protection (ICNIRP, 2010) and the Institute of Electrical and Electronics Engineers (IEEE, 2006)  
72 provide guidelines to limit the human exposure to time-varying electric, magnetic and  
73 electromagnetic field (ICNIRP, 2010; IEEE, 2006).

## 74 **2. WPT system for dairy cows**

75 We tested the WPT system presented by Minnaert et al., (2017) at the Flanders Research Institute  
76 for Agriculture, Fisheries and Food (ILVO) in Melle, Belgium. Fig. 1-a shows a cow in the feeding  
77 trough where the WPT system was installed. When the cow was eating, the transmitter located at  
78 the feeding trough transmitted energy to the receiver attached to the collar of the cow. The

79 transmitter coil (Fig. 1-b) had an oval shape of 27.0 cm x 13.5 cm and was installed on a 32.5 cm x  
80 15.6 cm x 0.6 cm layer of ferrite (3F4). The receiver coil (Fig.1-c) had an oval shape of 12.6 cm x  
81 9.6 cm with a 6.5 cm x 5.2 cm x 0.6 cm ferrite core. Both coils had 5 turns made of 1.5 mm<sup>2</sup> Cu wire.  
82 The optimal dimensions of the coils were experimentally determined for a maximum power transfer.  
83 The resonance frequency was 92 kHz. The electrical parameters of the TX and RX coils measured with  
84 an Agilent 4285A LCR meter at 92 kHz are listed in Table 1. More details about the system are  
85 available in Minnaert et al., (2017).

### 86 **3. Materials and Methods**

#### 87 3.1 Computational techniques and Quasi-Static (QS) approximation

88 In this study, the 3-D electromagnetic solver Sim4Life (Maiques, 2014) was used. For frequencies  
89 above 1 MHz, simulations were performed with the finite difference time domain (FDTD) method; for  
90 frequencies below 1 MHz, the quasi-static (QS) approximation using the finite element method (FEM)  
91 was employed to reduce the computational complexity and the simulation time (Laakso et al., 2015;  
92 Samoudi et al., 2016). The applicability of the QS approximation has been proven for human  
93 exposure to WPT systems for frequencies up to 10 MHz by Laakso et al. (2015).  
94 Instead of using a one-step method based on a full-wave analysis for the original problem all at once,  
95 a two-step process was used as explained in Park and Kim (2016). Using this method, the number of  
96 time steps can be considerably decreased due to rapid convergence within a time shorter than one  
97 full period, whereas the conventional method has to simulate several periods to reach the steady  
98 state. The first step is to obtain the EMFs generated from the WPT system in the absence of the  
99 cow's body. In the second step, the induced EMFs in the cow's body is calculated with a QS-FEM  
100 method by regarding the EMFs obtained in the previous step as the incident field to the cow's body.

## 3.2 Electromagnetic modeling of the WPT system and cow's body

### 3.2.1 Modeling of the WPT system

Fig. 2 shows the transmitter and the receiver coils of the WPT system as modelled in Sim4Life. Both coils were modelled with five turns of a perfect conductive  $1.5 \text{ mm}^2$  wire. The transmitter coil was installed on a rectangular ferrite (Fig. 2-a), while the receiver coil has a core ferrite with the same dimensions as the experimental coil. The relative permeability of the ferrite (i.e., 3F4) is 900 at 92 kHz (Matz et al., 2009).

### 3.2.2 Modelling of the cow's body

We used the homogeneous cow model developed by Benaissa et al. (2016b); for human body simulations, several anatomical models are available (Ackerman, 1998), , but no anatomical models exist for a cow's body. The cow's body was modelled as a homogeneous medium with the following dimensions: withers-tail 1.8 m, width 0.7 m, nose-tail 2.6 m, rump-hoof 1.4 m, stance (i.e., front-to-rear claws) 1.7 m, chest 0.8 m, withers (shoulder) height 1.4 m, and hook-bone width 0.6 m (Benaissa et al., 2016b). The numerical cow model is composed of muscle tissue with the dielectric properties at the operating frequency of the system (92 kHz); conductivity  $\sigma=0.35 \text{ S/m}$  and relative permittivity  $\epsilon_r=8097$  (Gabriel et al., 1996). Uniform rectilinear meshes were applied to easily discretize the complex anatomical models with a voxel size of 2 mm along x, y, and z direction.

## 3.3 Experimental setup for the validation of the WPT system

To validate the numerical model of the WPT system, we compared simulated free-space magnetic fields emitted by the WPT system with the measured fields. The peak value of the magnetic field was measured with the EHP-50 electric and magnetic field probe (Narda safety test solutions, Milan, Italy). The isotropy error of this probe for the magnetic field is  $\pm 0.8 \text{ dB}$  at 1 MHz and its frequency response is  $\pm 0.8 \text{ dB}$  over a frequency range from 9 kHz to 30 MHz. Field sensors (radius 46 mm) and electronic measuring circuitry were fitted into a housing of  $92 \times 92 \times 109 \text{ mm}^3$  in size. The probe was mounted on a plastic mast at 1 m above the ground as shown in Fig. 3-a. We, first, measured without the receiver coil as shown in Fig. 3-b. The transmitter was kept in a fixed position. Then, the field

127 analyzer was positioned at different distances from the TX coil (i.e., 2, 5, 10, 15, 20 cm). The center  
128 point of the probe was aligned with the horizontal axis of the coil. Next, we measured with both  
129 transmitter and receiver. In this case, the H-field was measured 5 cm from the RX coil for different  
130 TX-RX separations (i.e., 10, 15, 20 cm) as shown in Fig. 3-c. The E-field was not considered in the  
131 validation since the dominant coupling with the body is due to the magnetic field (Kuster and  
132 Balzano, 1992).

133 The transmitter was powered by a DC supply with a DC voltage of 12.00 V and a DC current of 305  
134 mA, corresponding with an active input power of 3.66 W. This input power was converted with an  
135 efficiency of 27.3 % to a transmitting power of 1.0 W at the transmitter coil. The peak voltage and  
136 current in the transmitter coil were 42.0 V and 6.32 A, respectively. The AC power received at the  
137 receiver coil is given in the Table 2, as well as the coupling factors for the different distances. Peak  
138 voltage and current in the receiver coil at 10 cm distance were 7.5 V and 2.9 A, respectively. For the  
139 simulations, a current of 7.5 A (peak value) was applied to the TX coil. The received current at the RX  
140 coil as well as the coupling factor could not be calculated by the simulator.

#### 141 3.4 Exposure scenarios

142 To mimic realistic exposure scenarios, the WPT system was located at different distances below the  
143 cow's neck. Experiments in Minnaert et al., (2017) showed that the distance between the receiver  
144 coil and the cow's neck could vary from 2 cm up to 5 cm, whereas the distance between the  
145 transmitter coil and the cow's neck could vary from 10 cm up to 20 cm. Therefore, the RX and TX in  
146 the simulations were set at d1 (2.5 and 5 cm) and d2 (10, 15, and 20 cm), respectively, from the  
147 cow's body (Fig. 4). The values of d1 and d2 for each scenario are listed in Table 3.

#### 148 3.5 ICNIRP and IEEE fields evaluation and limits

149 As guidelines for animal exposure to EMF lack, guidelines for human exposure were used in this  
150 study. The guidelines protect against stimulation effects for frequencies up to 10 MHz and protect  
151 against thermal effects for frequencies between 100 kHz and 10 GHz. Protection against stimulation  
152 effects is in terms of the 99th percentile of the internal electric field; protection against thermal

153 effects is in terms of the specific absorption rate (SAR). Since the operating frequency of the WPT  
154 system is around 100 kHz, both the internal electric field and the SAR were considered in this study.  
155 The compliance of the WPT system with international EMF exposure guidelines was investigated  
156 using the parameters from these standards. ICNIRP 2010 (ICNIRP, 2010) calculates the induced  
157 electric field as a vector average within a contiguous tissue cubic volume of  $2 \times 2 \times 2 \text{ mm}^3$ . It suggests  
158 using the 99th percentile value of the calculated internal electric field for the compliance with the  
159 guidelines. However, in the IEEE standard (IEEE, 2006), the internal electric field is specified as an  
160 arithmetic average of electric fields projected onto a straight line segment of 5 mm length oriented in  
161 any direction within the tissue. We note that for IEEE standard, the exposure limits for uncontrolled  
162 environments were considered.

## 163 **4. Results**

### 164 4.1 WPT system validation

165 Fig. 5 shows the measured and the simulated H-fields for the TX coil alone case (Fig.3 –b). For all  
166 cases (middle, right, and left sides), agreement between the measurements and simulations was  
167 achieved, especially for distances greater than 5 cm from the TX coil. At 2 cm, the probe is close to  
168 the wires of the coils, which could influence the field generated by the coil. Table 4 lists the  
169 measured and simulated H-field for the full WPT system (Fig. 3-c). Also in this case, the results show  
170 good agreement between the measurements and simulations with differences less than 2 A/m.

171 The maximum, the minimum, and the average of the relative and absolute errors between the  
172 measured and simulated H-field samples are listed in Table 5. The relative error varies between  
173 2.25 % and 9.92 % with an average of 5.87 % and the absolute error varies between 0.07 A/m and  
174 7.95 A/m with an average of 1.67 A/m. The maximum errors occurred in close proximity of the coils  
175 (2 cm); however, the average relative error was less than 6 %.

## 4.2 E-field distribution

176  
177 Fig. 6 shows the internal electric field (in dB normalized to 0.5 V/m) in the cow for all investigated  
178 scenarios (Section 3.4) for an input power of 1 W. Scenario I showed the largest internal electric  
179 fields (0.49 V/m), whereas scenario VI showed the minimum values (0.11 V/m). This is due to the  
180 configuration of the TX coil playing the major role in the electric field induction in the cow. In  
181 scenario I, the TX is at its nearest location to the cow neck while it is at its furthest position from the  
182 cow in scenario VI. The distance between RX coil and the cow did not have much effect on the  
183 induced electric field (differences less than 10%), when the TX coil was at a fixed distance from the  
184 cow's body.

## 4.3 $E_{\max}$ and $E_{99\%}$ for ICNIRP 2010 and IEEE 2005

185  
186 In order to study the coils compliance with the basic restrictions (ICNIRP, 2010; IEEE, 2006), the  
187 internal induced electric fields were calculated using the maximum value and the 99<sup>th</sup> percentile  
188 value. ICNIRP 2010 recommends a maximum value of 13.5 V/m for internal E-field at 92 kHz, while  
189 the IEEE guidelines recommend a maximum of 20.9 V/m for internal E-field. Table 6 lists the  
190 calculated electric field in the cow model for the considered scenarios. The highest induced electric  
191 field (Table 6) occurs for the scenarios I and IV (maximum  $E_{99\%}$  of 0.21 V/m and 0.20 V/m for I and IV,  
192 respectively). For these scenarios, the distance  $d_2$  is at its minimum ( $d_2=10$  cm) making the TX coil at  
193 the nearest position to the cow. The lowest  $E_{99\%}$  (0.066 V/m) occurred when both the TX and RX are  
194 at the furthest position from the cow ( $d_1 = 5$  cm and  $d_2 = 20$  cm). A 3.5 % difference between  
195 scenarios I and IV (changing only the RX position) compared to a 48.5 % difference between  
196 scenarios I and II (changing only the TX position) shows that TX coil has the greater effect on the  $E_{99\%}$   
197 compared to the RX coil. The great effect of the TX coil on the induced electric field was also reported  
198 and discussed in section 4.2. For an input power of 1 W, the limits were not exceeded for both  
199 ICNIRP and IEEE guidelines.



#### 4.4 Local and whole-body SAR

To investigate the thermal effect of the WPT system and its compliance with ICNIRP and IEEE guidelines, the peak localized SAR ( $SAR_{1g}$  and  $SAR_{10g}$ ) and whole-body SAR ( $SAR_{wb}$ ) were computed for the six exposure scenarios defined in section 3.4. Table 7 lists the obtained values for an input power of 1 W. The induced whole-body SAR values vary between 7.11  $\mu\text{W}/\text{kg}$  (Scenario I) and 0.39  $\mu\text{W}/\text{kg}$  (scenario VI). For the local SAR ( $SAR_{1g}$  and  $SAR_{10g}$ ), the obtained values were higher than the whole-body SAR values.  $SAR_{10g}$  varied between 44.63  $\mu\text{W}/\text{kg}$  (scenario I) and 2.58  $\mu\text{W}/\text{kg}$  (scenario VI). Similarly,  $SAR_{1g}$  varied between 56.76  $\mu\text{W}/\text{kg}$  and 3.12  $\mu\text{W}/\text{kg}$ . Similar to what was found for the electric field, the TX coil has a greater effect on the SAR values than the RX coil.

### 5. Discussion

This work is a first step to study the exposure of the cow's body to WPT systems. After the validation of the experimental WPT system, the induced electric field and the SAR values were computed based on Sim4Life simulations for different separations between the source (transmitter and receiver coils) and the cow's body. The induced electric field depended mainly on the distance between the transmitter and the cow's body, with variations exceeding 5 dB between scenario I and scenario VI. However, the distance between the receiver and the cow's body had less influence (10%). In comparison to human exposure limits (13.5 V/m for ICNIRP 2010 and 20.9 V/m for IEEE 2006), the induced electric field values were lower than the limits for all the investigated scenarios. This could be explained by the low input power used for the simulations. To deploy the WPT system in barns, the values of the induced electric field computed in this paper could be used to derive the maximum allowable input power that has to be respected to stay under the exposure limit. For the SAR, the obtained values were lower than 1% of the limit (0.08 for  $SAR_{wb}$ , 1.6 W/kg for  $SAR_{1g}$  and 2 W/kg for  $SAR_{10g}$ ). This means that the thermal effect of the WPT system is very limited at that frequency (92 kHz). This is because the operating frequency is slightly below 100 kHz. Therefore, the maximum allowable transmit power at which the SAR limit is reached is in the order of several kW, which is in our case, far above the range of input power used in wireless power transfer system in a dairy barn

226 (in W). Above 100 kHz, ICNIRP specifies its basic restriction to prevent whole-body heat stress and  
227 excessive localized tissue heating in terms of SAR. Therefore, the induced electric field restriction is  
228 the most stringent exposure limit for the evaluation of the WPT coils. The same conclusions were  
229 drawn in (Park, 2017) about human exposure to WPT systems. In that work, SAR<sub>wb</sub> values between  
230 0.15 and 1.31  $\mu\text{W}/\text{kg}$  were reported for an input power of 1 W. As stated in the IEEE C95.1-2005  
231 standard (IEEE, 2006), guidelines (IEEE and ICNIRP) provide recommendations to minimize aversive or  
232 painful electrostimulation in the frequency range of 3 kHz to 5 MHz and to protect against adverse  
233 heating in the frequency range of 100 kHz to 300 GHz. Below 100 kHz, the aversive or painful  
234 electrostimulation is the effect being minimized. At low frequencies, exposures are assessed in terms  
235 of instantaneous fields or currents (internal electric field used in our study). Above 100 kHz, there  
236 can be a sensation of heat, which is not considered adverse. Above 100 kHz, exposures are assessed  
237 with reference to an average time that varies with frequency (SAR used in our study). The frequency  
238 of 100 kHz nominally represents a “thermal crossover” below which electrostimulation effects  
239 dominate, and above which thermal effects dominate for continuous wave exposure (IEEE, 2006).  
240 This justifies why the SAR values, mainly used to minimize adverse heating effects, are negligible  
241 compared to the limits for the considered system (lower than 1% of the limit). SAR values will be  
242 much higher (compared to limits) in the MHz range, and the opposite will happen for the internal  
243 electric field.

244 The homogeneous body of the cow phantom was one limitation of the present study. A  
245 heterogeneous model - including other tissues than muscle only- will give more realistic values for  
246 the exposure metrics. Also, this study considers only the case when the centres of the transmitter  
247 and receiver coil are perfectly aligned (i.e., optimal power transfer). When the coils are misaligned,  
248 either laterally or angularly, the magnetic flux through the receiver coil will decrease, leading to a  
249 lower power transfer (Fotopoulou and Flynn, 2011). However, this may increase the SAR values as  
250 reported in (Park, 2017) The analysis performed in that work showed that the worst-case exposure

251 scenario (higher values of the SAR) generally occurred in the misalignment case. Therefore, further  
252 research is required in this direction.

## 253 **6. Conclusions and future work**

254 In this paper, we investigated cow exposure to EMF of a WPT system operating at 92 kHz. After the  
255 experimental validation of the WPT source, the induced fields in the cow's body were numerically  
256 computed using 3-D electromagnetic software (Sim4Life). Cow exposure depends mainly on the  
257 separation between the transmitter and cow's body; the distance between the receiver and the  
258 cow's body has less influence (10%) on the exposure metrics. We also observed that, unlike the  
259 stimulation effect, the thermal effect, evaluated by the specific absorption rate, of the WPT system  
260 on the cow's body is very limited. Therefore, the induced electric field will mainly define the final  
261 acceptable input power level. In future works, the effect of the cow's body posture, the inner  
262 anatomy (i.e., heterogeneous phantom), and off-centering effect of the coils should be taken in  
263 consideration. Also, the WPT systems operating in the MHz range should be investigated, since the  
264 stimulation effect does not occur in this range. Finally, the influence of the exposure to the cows'  
265 behavior (i.e., feeding) and production (i.e., milk) should be investigated. This is a mandatory step  
266 before integrating the system in the dairy farm.

## 267 **7. Acknowledgments**

268 This work was executed within MoniCow, a research project bringing together academic researchers  
269 and industry partners. The MoniCow project was co-financed by imec (iMinds) and received project  
270 support from Flanders Innovation & Entrepreneurship.

## 271 **8. References**

- 272 Ackerman, M.J., 1998. The visible human Project: A resource for anatomical visualization, in: *Studies*  
273 *in Health Technology and Informatics*. pp. 1030–1032. doi:10.3233/978-1-60750-896-0-1030
- 274 Algers, B., Hultgren, J., 1987. Effects of long-term exposure to a 400-kV, 50-Hz transmission line on  
275 *estrous and fertility in cows*. *Prev. Vet. Med.* 5, 21–36. doi:10.1016/0167-5877(87)90003-1
- 276 Andersson, L.M., Okada, H., Miura, R., Zhang, Y., Yoshioka, K., Aso, H., Itoh, T., 2016. *Wearable*

277 wireless estrus detection sensor for cows. *Comput. Electron. Agric.* 127, 101–108.  
278 doi:10.1016/j.compag.2016.06.007

279 Benaissa, S., Plets, D., Tanghe, E., Verloock, L., Martens, L., Hoebeke, J., Sonck, B., Tuytens, F.A.M.,  
280 Vandaele, L., Stevens, N., Joseph, W., 2016a. Experimental characterisation of the off-body  
281 wireless channel at 2.4GHz for dairy cows in barns and pastures. *Comput. Electron. Agric.* 127,  
282 593–605. doi:10.1016/j.compag.2016.07.026

283 Benaissa, S., Plets, D., Tanghe, E., Vermeeren, G., Martens, L., Sonck, B., Tuytens, F.A.M., Vandaele,  
284 L., Hoebeke, J., Stevens, N., Joseph, W., 2016b. Characterization of the on-body path loss at 2.45  
285 GHz and energy efficient WBAN design for dairy cows. *IEEE Trans. Antennas Propag.* 11, 4848–  
286 4858. doi:10.1109/TAP.2016.2606571

287 Bhatnagar, V., Owende, P., 2015. Energy harvesting for assistive and mobile applications. *Energy Sci.*  
288 *Eng.* doi:10.1002/ese3.63

289 Burchard, J.F., Nguyen, D.H., Block, E., 1998. Progesterone concentrations during estrous cycle of  
290 dairy cows exposed to electric and magnetic fields. *Bioelectromagnetics* 19, 438–43.

291 Burda, H., Begall, S., Cerveny, J., Neef, J., Nemecek, P., 2009. Extremely low-frequency electromagnetic  
292 fields disrupt magnetic alignment of ruminants. *Proc. Natl. Acad. Sci.* 106, 5708–5713.  
293 doi:10.1073/pnas.0811194106

294 Erdreich, L.S., Alexander, D.D., Wagner, M.E., Reinemann, D., 2009. Meta-analysis of stray voltage on  
295 dairy cattle. *J. Dairy Sci.* 92, 5951–5963. doi:10.3168/jds.2008-1979

296 Fotopoulou, K., Flynn, B.W., 2011. Wireless power transfer in loosely coupled links: Coil misalignment  
297 model. *IEEE Trans. Magn.* 47, 416–430. doi:10.1109/TMAG.2010.2093534

298 Gabriel, S., Lau, R.W., Gabriel, C., 1996. The dielectric properties of biological tissues: III. Parametric  
299 models for the dielectric spectrum of tissues. *Phys. Med. Biol.* 41, 2271–2293.  
300 doi:10.1088/0031-9155/41/11/003

301 González, L.A., Bishop-Hurley, G.J., Handcock, R.N., Crossman, C., 2015. Behavioral classification of  
302 data from collars containing motion sensors in grazing cattle. *Comput. Electron. Agric.* 110, 91–  
303 102. doi:10.1016/j.compag.2014.10.018

304 Hillman, D., Stetzer, D., Graham, M., Goeke, C.L., Mathson, K.E., Vanhorn, H.H., Wilcox, C.J., 2013.  
305 Relationship of electric power quality to milk production of dairy herds - field study with  
306 literature review. *Sci. Total Environ.* 447, 500–14. doi:10.1016/j.scitotenv.2012.12.089

307 ICNIRP, 2010. Guidelines for limiting exposure to time-varying electric and magnetic fields (1 Hz to  
308 100 kHz). *Health Phys.* 99, 818–36. doi:10.1097/HP.0b013e3181f06c86

309 IEEE, 2006. IEEE Standard for Safety Levels With Respect to Human Exposure to Radio Frequency  
310 Electromagnetic Fields, 3 kHz to 300 GHz, IEEE Std C95.1-2005 (Revision of IEEE Std C95.1-  
311 1991). doi:10.1109/IEEESTD.2006.99501

312 Kuster, N., Balzano, Q., 1992. Energy Absorption Mechanism by Biological Bodies in the Near Field of  
313 Dipole Antennas Above 300 MHz. IEEE Trans. Veh. Technol. 41, 17–23. doi:10.1109/25.120141

314 Laakso, I., Shimamoto, T., Hirata, A., Feliziani, M., 2015. Quasistatic approximation for exposure  
315 assessment of wireless power transfer. IEICE Trans. Commun. E98B, 1156–1163.  
316 doi:10.1587/transcom.E98.B.1156

317 Löscher, W., 2003. Die auswirkungen elektromagnetischer felder von mobilfunksendeanlagen auf  
318 leistung, gesundheit und verhalten landwirtschaftlicher nutztiere: Eine bestandsaufnahme.  
319 Prakt. Tierarzt 84, 850–863.

320 Maiques, M.M., 2014. Sim4Life: A Simulation Platform for Life Sciences and Medtech Applications.  
321 Eur. Cells Mater. 27.

322 Matz, R., Gotsch, D., Karmazin, R., Manner, R., Siessegger, B., 2009. Low temperature cofirable MnZn  
323 ferrite for power electronic applications. J. Electroceramics 22, 209–215. doi:10.1007/s10832-  
324 007-9334-9

325 Minnaert, B., Thoen, B., Plets, D., Joseph, W., Stevens, N., 2017. Optimal energy storage solution for  
326 an inductively powered system for dairy cows, in: WPTC 2017 - Wireless Power Transfer  
327 Conference. doi:10.1109/WPT.2017.7953805

328 Neethirajan, S., 2017. Recent advances in wearable sensors for animal health management. Sens.  
329 Bio-Sensing Res. doi:10.1016/j.sbsr.2016.11.004

330 Nguyen, C.M., Kota, P.K., Nguyen, M.Q., Dubey, S., Rao, S., Mays, J., Chiao, J.C., 2015. Wireless power  
331 transfer for autonomous wearable neurotransmitter sensors. Sensors (Switzerland) 15, 24553–  
332 24572. doi:10.3390/s150924553

333 Park, S., Kim, M., 2016. Numerical Exposure Assessment Method for Low Frequency Range and  
334 Application to Wireless Power Transfer. PLoS One 11. doi:ARTN  
335 e016672010.1371/journal.pone.0166720

336 Park, S.W., 2017. Misaligned Effect and Exposure Assessment for Wireless Power Transfer System  
337 Using the Anatomical Whole-Body Human Model 77, 19–28.

338 Rutten, C.J., Kamphuis, C., Hogeveen, H., Huijps, K., Nielen, M., Steeneveld, W., 2017. Sensor data on  
339 cow activity, rumination, and ear temperature improve prediction of the start of calving in dairy  
340 cows. Comput. Electron. Agric. 132, 108–118. doi:10.1016/j.compag.2016.11.009

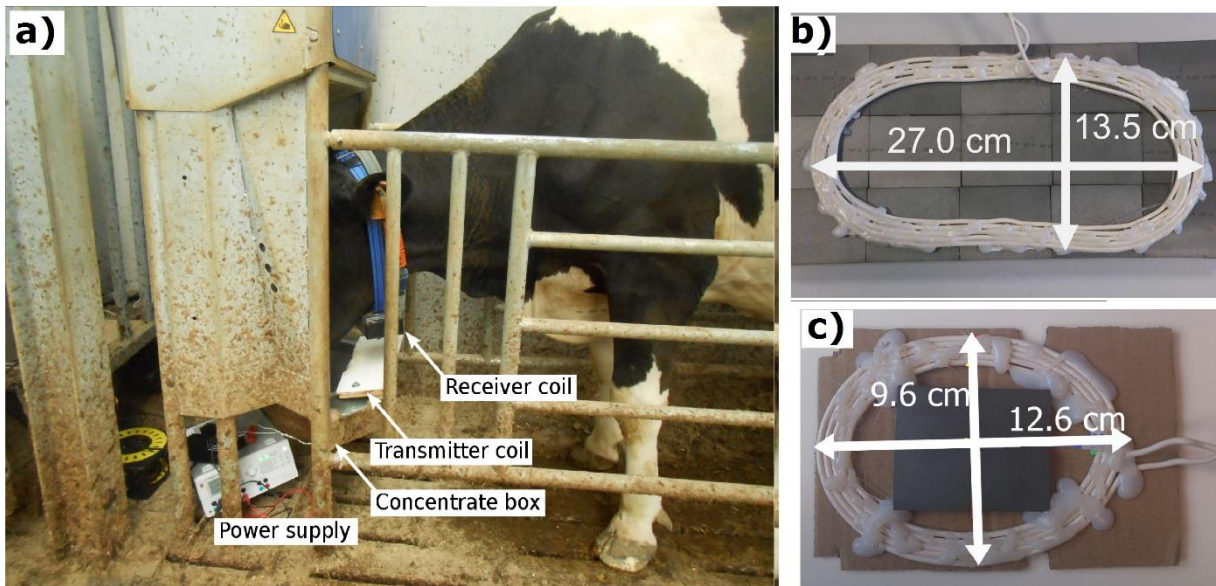
341 Samoudi, A.M., Vermeeren, G., Tanghe, E., Van Holen, R., Martens, L., Josephs, W., 2016. Numerically  
342 simulated exposure of children and adults to pulsed gradient fields in MRI. *J. Magn. Reson.*  
343 *Imaging* 44, 1360–1367. doi:10.1002/jmri.25257

344 Van Nuffel, A., Zwertvaegher, I., Van Weyenberg, S., Pastell, M., Thorup, V.M., Bahr, C., Sonck, B.,  
345 Saeys, W., 2015. Lameness detection in dairy cows: Part 2. Use of sensors to automatically  
346 register changes in locomotion or behavior. *Animals*. doi:10.3390/ani5030388

347

348 **9. Figure captions**

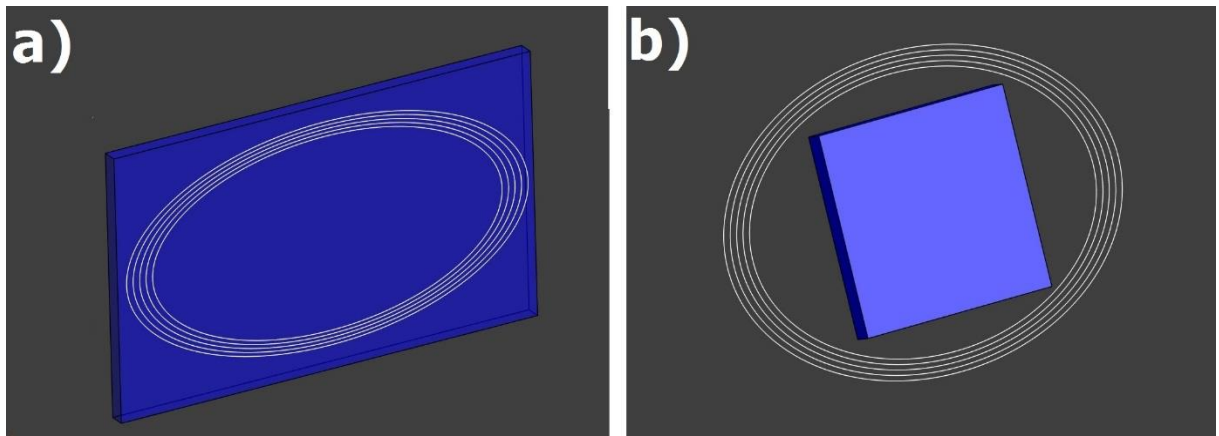
349 **Fig. 1.** A cow in the feeding trough where the WPT is installed (a). When the cow is feeding, the  
350 transmitter coil (b) transmits energy to the receiver coil (c).



351

352

353 **Fig. 2.** Numerical model of the WPT system in the simulation software Sim4Life. Transmitter (a),  
354 receiver (b). The transmitter coil was installed on a 32.5 cm x 15.6 cm x 0.6 cm layer of ferrite and the  
355 receiver coil had a 6.5 cm x 5.2 cm x 0.6 cm ferrite core.

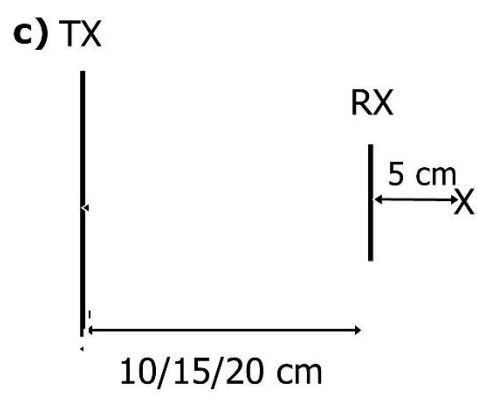
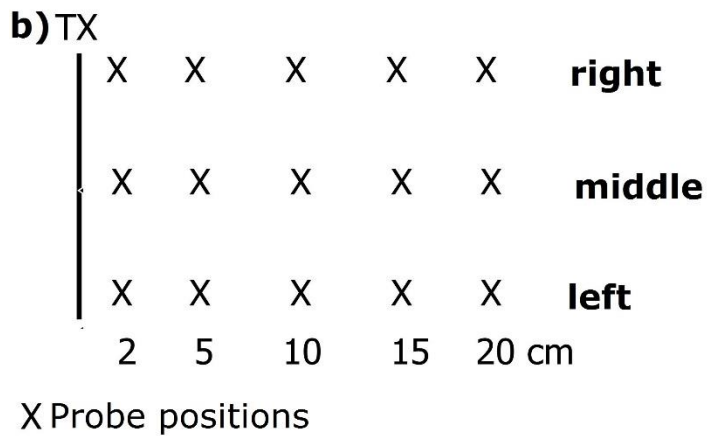
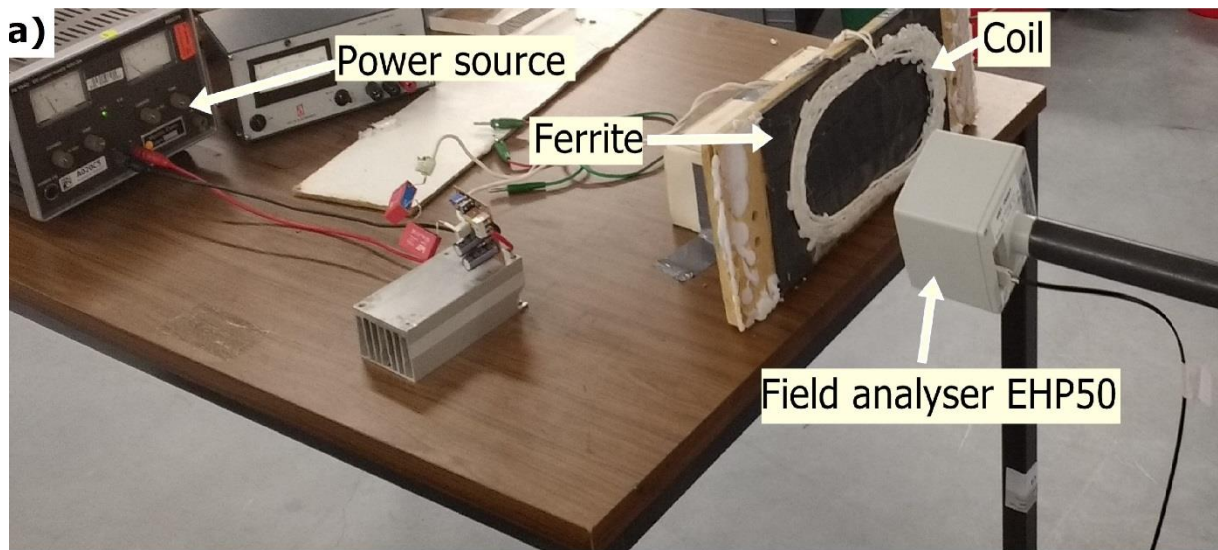


356

357



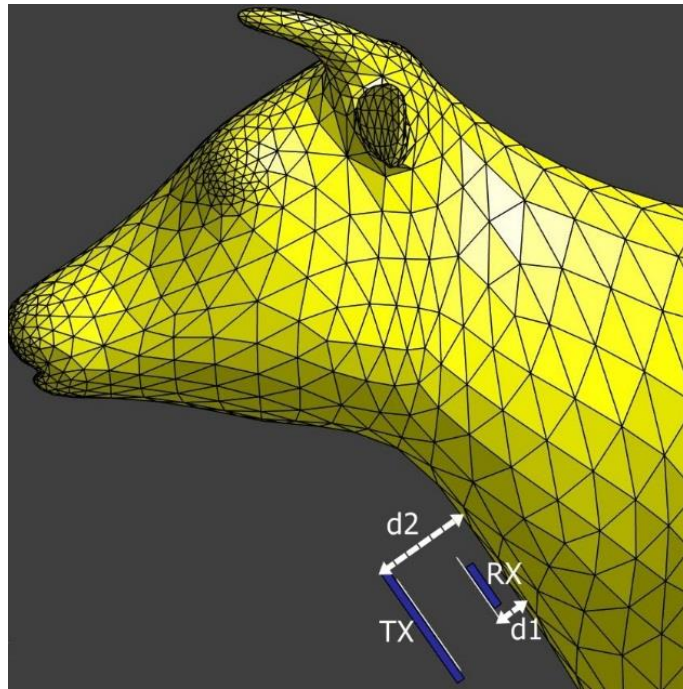
358 **Fig. 3.** Experimental setup for the validation of the numerical WPT model (a). The H-field was  
 359 measured and calculated at different positions with TX alone (b) and TX and RX together (c).



360

361

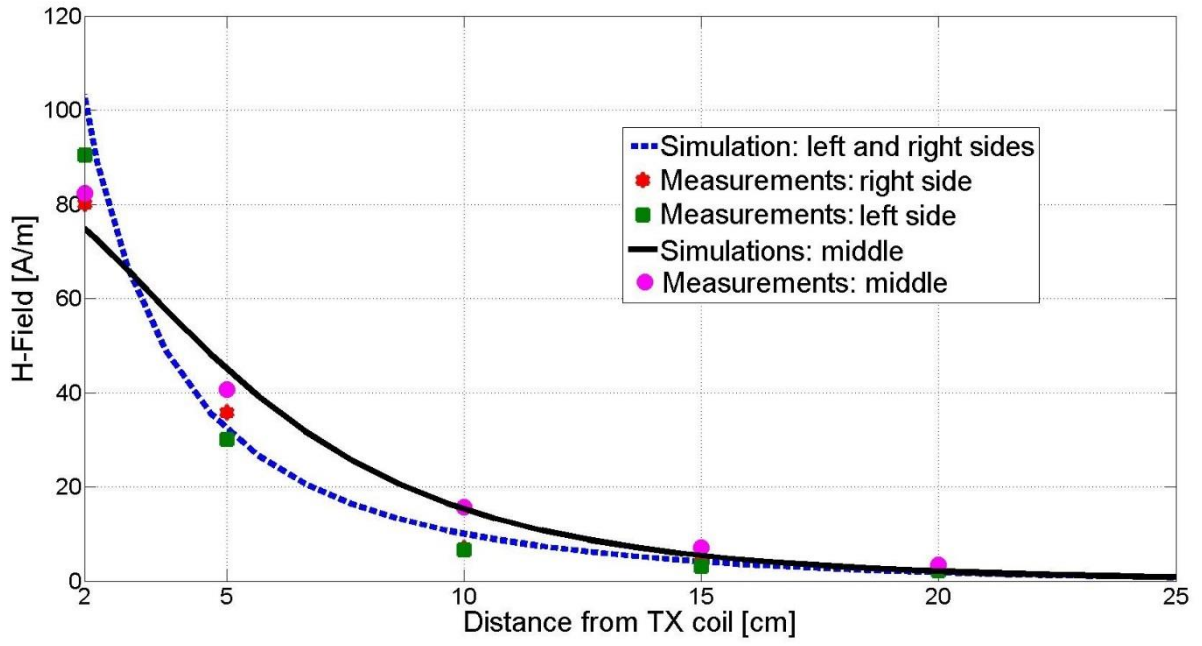
362 **Fig. 4.** Exposure scenarios: the RX and TX were set at d1 (2.5 and 5 cm) and d2 (10, 15, and 20 cm),  
363 respectively, from the cow's body.



364

365

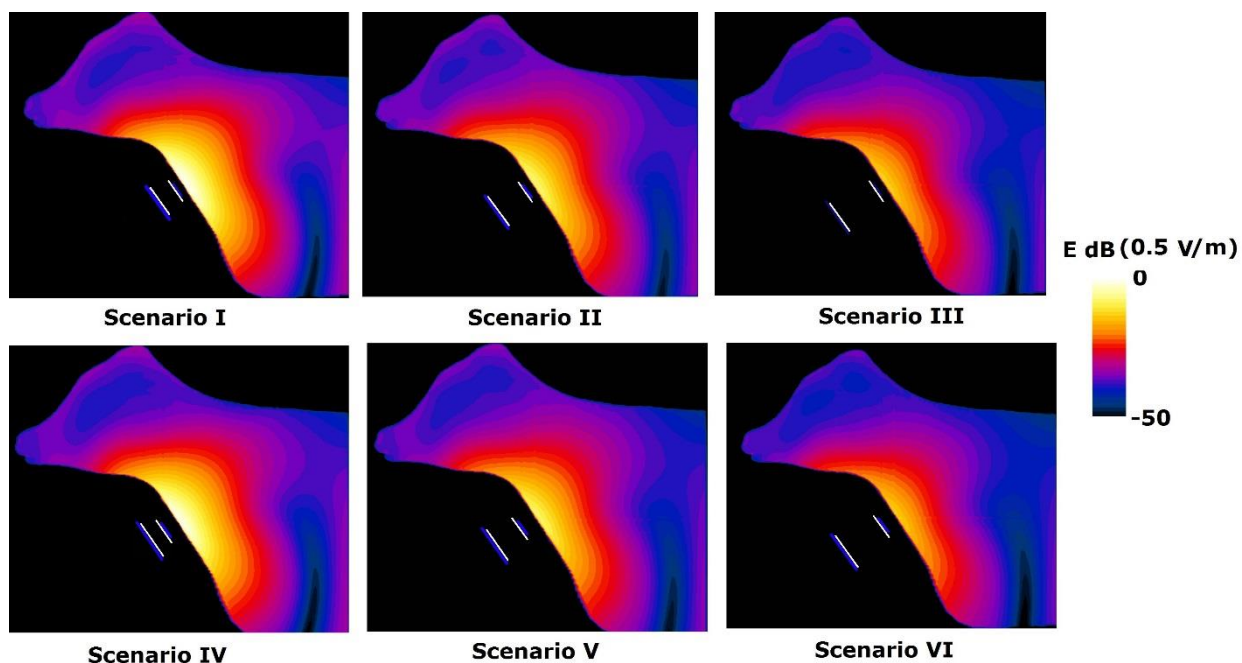
366 **Fig. 5.** Simulated and measured H-field values from the TX coil alone in the middle and in the left  
367 and right sides of the horizontal axis. (Middle, left, and right are defined in Fig. 3-b).



368

369

370 **Fig. 6.** Distribution of the internal electric field in the cow's body for the six scenarios defined in  
371 Table 3 for an input current (peak) of 7.5 A (input power of 1 W). The lines under the cow's neck are  
372 the transmitter and the receiver of the WPT system.



373

374

375 **10. Table captions**

	Transmitter coil (TX)	Receiver coil (RX)
Inductance L	15 $\mu$ H	4.71 $\mu$ H
Quality factor Q	170	53
Resistance R	0.05 $\Omega$	0.05 $\Omega$

376 Table 1. The electrical parameters of the TX and RX coils measured with an Agilent 4285A LCR meter  
377 at 92 kHz.

378

Distance TX-RX	Received power at the receiver coil	Magnetic link efficiency coil to coil.	Coupling factor k
10 cm	430 mW	43.0 %	4.8%
15 cm	185 mW	18.5 %	2.7%
20 cm	35 mW	3.5 %	1.3%

379 Table 2. The measured AC power received at the receiver coil for each TX-RX separation

380

381

		Distance d2 [cm]		
		10	15	20
Distance d1 [cm]	2.5	Scenario I	Scenario II	Scenario III
	5	Scenario IV	Scenario V	Scenario VI

382 **Table 3.** The distances of the transmitter coil (d1) and the receiver coil (d2) above the cow's body for  
383 the investigated scenarios.

384

TX-RX separation [cm]	10	15	20
H- field Measurements [A/m]	24.96	10.91	5.06
H- field Simulations [A/m]	23.22	10.36	5.57

385 **Table 4.** Simulated and measured H-Field values for TX and RX together.

386

	Maximum	Minimum	Average
Relative error <sup>1</sup> [%]	9.92	2.25	5.87
Absolute error <sup>2</sup> [A/m]	7.95	0.07	1.64

387 **Table 5.** Simulation versus measurements relative and absolute errors

388 <sup>1</sup> Difference calculated as follows  $| (Simulation-Measurement)/ Simulation | *100$ .

389 <sup>2</sup> Error field calculated as follows  $|Simulation - Measurement |$ .

390

391

Scenarios	ICNIRP		IEEE	
	$E_{\max}$ (V/m)	$E_{99\%}$ (V/m)	$E_{\max}$ (V/m)	$E_{99\%}$ (V/m)
I (d1=2.5 cm, d2=10 cm)	0.491	0.208	0.466	0.208
II (d1=2.5, d2=15)	0.224	0.107	0.213	0.107
III (d1=2.5, d2=20)	0.112	0.072	0.108	0.072
IV (d1=5, d2=10)	0.445	0.201	0.433	0.201
V (d1=5, d2=15)	0.214	0.097	0.207	0.097
VI (d1=5, d2=20)	0.110	0.066	0.101	0.066

392 **Table 6.**  $E_{\max}$  and  $E_{99\%}$  of the simulated E-field distribution for an input current (peak) of 7.5 A  
393 (input power of 1 W) for the six scenarios explained in Table 3.

394

Scenarios	SAR <sub>wb</sub> ( $\mu$ W/kg)	SAR <sub>10g</sub> ( $\mu$ W/kg)	SAR <sub>1g</sub> ( $\mu$ W/kg)
I (d1=2.5 cm, d2=10 cm)	7.11	44.63	56.76
II (d1=2.5, d2=15)	2.65	9.87	12.34
III (d1=2.5, d2=20)	0.42	2.61	3.17
IV (d1=5, d2=10)	6.03	44.30	56.48
V (d1=5, d2=15)	1.53	9.77	12.22
VI (d1=5, d2=20)	0.39	2.58	3.12

395 **Table 7.** SAR statistics in ( $\mu$ W/kg) for an input current (peak) of 7.5 A (input power of 1 W) for the  
396 six scenarios explained in Table 3.

397